PNAS
www.pnas.org

Supplementary Information for

Viable cyanobacteria in the deep continental subsurface

Fernando Puente-Sánchez, Alejandro Arce-Rodríguez, Monika Oggerin, Miriam García-Villadangos, Mercedes Moreno-Paz, Yolanda Blanco, Nuria Rodríguez, Laurence Bird, Sara Lincoln, Fernando Tornos, Olga Prieto-Ballesteros, Katherine H. Freeman, Dietmar H. Pieper, Kenneth N. Timmis, Ricardo Amils, Víctor Parro

Fernando Puente-Sánchez
Email: fpuente@cnb.csic.es

This PDF file includes:

Supplementary Text
Figs. S1 to S6
Tables S1 to S2
Captions for datasets S1 to S2
References for SI reference citations

Other supplementary materials for this manuscript include the following:

Datasets S1 to S2

www.pnas.org/cgi/doi/10.1073/pnas.1808176115

Supplementary Text

A metabolically versatile microbial community in the Iberian Pyrite Belt deep subsurface. The non-cyanobacterial organisms found in samples 420 and 607 (**Fig. 1B; SI Appendix, Data S2**) might be syntrophic with cyanobacteria (**SI Appendix, Fig. S5**), as is common in biological crusts (*1*). In particular, fungi are metabolically versatile and adept at penetrating rocks to access their internal resources, and increase the space available for colonization (*2*). We found laccases and peroxidases in the fungal fraction of our metagenomes, but no pathways for aromatic compounds degradation, suggesting that they are not able to grow on buried, recalcitrant organic matter on their own. However, the alphaproteobacteria showed nearly-complete pathways for the degradation of aromatic compounds, such as lignin or kerogen monomers (**SI Appendix, Fig. S6**). While some steps in such pathways are oxygen-dependent, small amounts of hydrogen peroxide – which yields oxygen via catalase – might be produced in the IPB subsurface by the reaction of water with defect surface sites on pyrite crystals (*3*). Fungi and alphaproteobacteria might thus cooperate in the degradation of recalcitrant organic matter, with the fungus being able to catalyze the breakdown of recalcitrant organic matters into smaller subunits, and the alphaproteobacterium being able to degrade the resulting compounds (**SI Appendix, Fig. S5**). Indeed, tight associations between ascomycota and alphaproteobacteria have been observed before in lignin degrading consortia (*4*). The monomers resulting from the depolymerization of recalcitrant organic matter could also be used as extracellular acceptors by cyanobacteria or other organisms. Another potential metabolism for alphaproteobacteria could be hydrogenotrophy, using nitrate or oxygen as the electron acceptors (*5*). Bacteroidetes, on the other hand, are specialized in the hydrolysis of complex carbohydrates, and could be feeding on cyanobacterial extracellular polysaccharides (EPS) as reported in other microbial mats (*6*). The EPS secreted by cyanobacteria would not only be a carbon source for heterotrophs, but also facilitate colonization by other organisms by protecting them from desiccation (*7*). Our results point at the existence of a metabolically coupled community in the deep subsurface of the IPB, in which cooperation and specialization are key to survival in the harsh conditions of the deep biosphere.

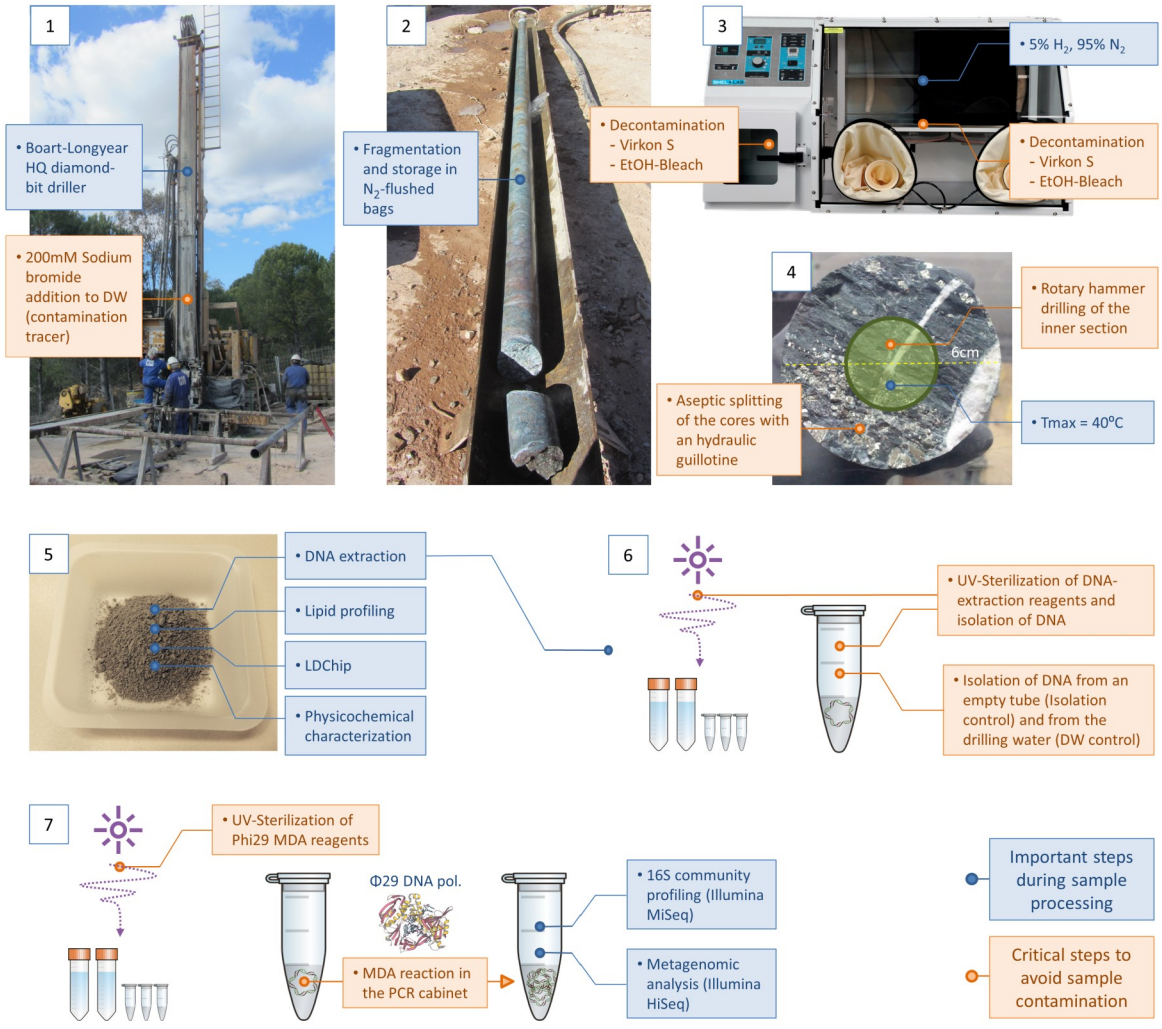

Fig. S1

Experimental setup from the extraction of IPB rock cores to the processing of the samples. Special care was taken in the steps in orange. 1) Drilling of the IPB. 2) Extraction and fragmentation of the rock cores. 3) The rock cores were transported to a sterilized anaerobic chamber. 4) The innermost part of the rock core was carefully drilled, checking constantly that the core temperature was not higher than 40ºC. 5) The core powder and shards were used for biological and physicochemical characterization. 6) DNA from the samples was extracted using UV-sterile components and reagents in an UV-sterile cleanbench. 7) The low amounts of DNA were amplified by means of multiple displacement amplification (MDA) using UV-sterile components and reagents in an UV-sterile PCR cabinet.

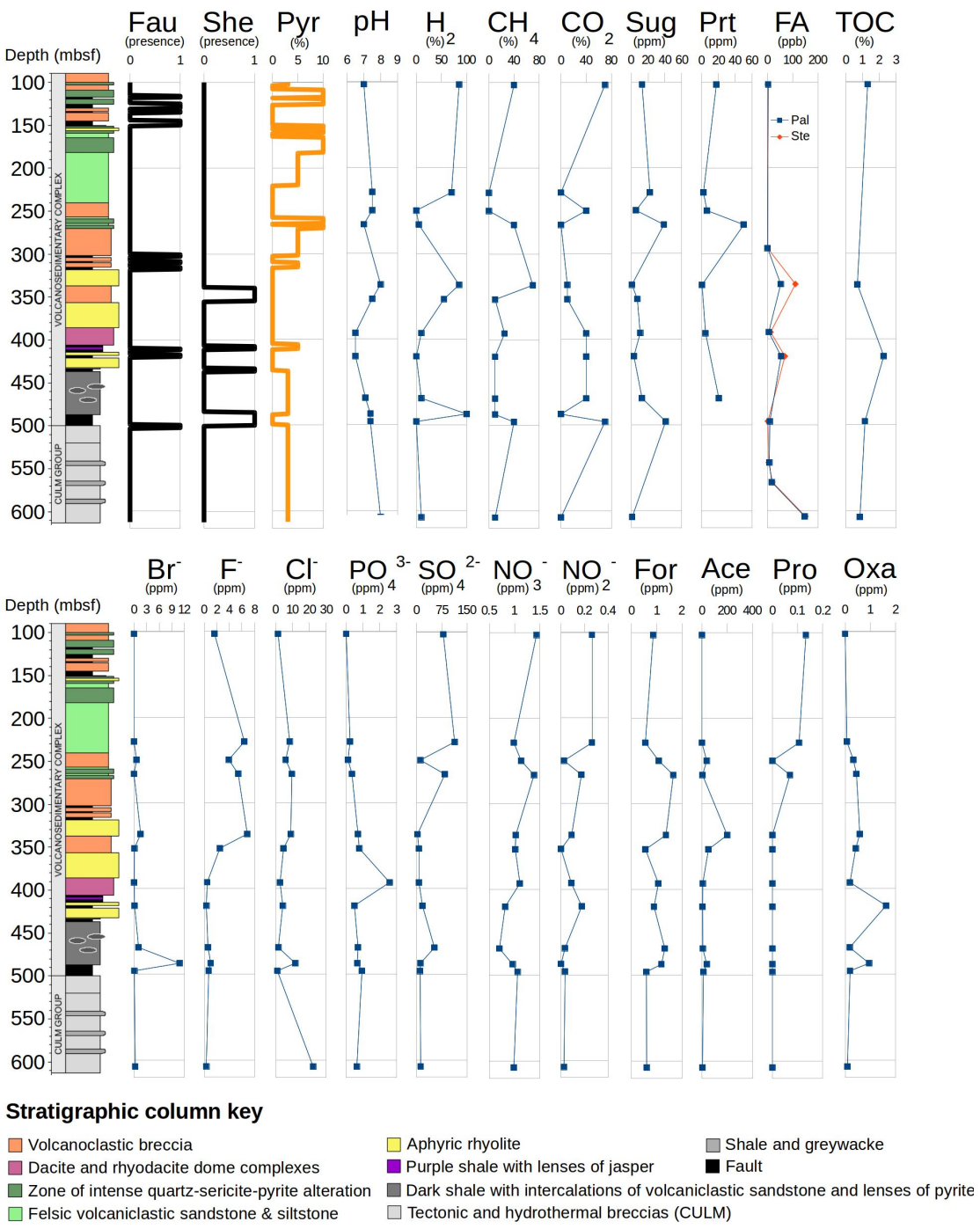

Fig. S2

Geological, physicochemical and organic compound profiling of borehole BH10. Abbreviations: Fau, faults; She, shears; Pyr, pyrite content; Sug, total sugars; Prt, total proteins; FA, fatty acids; Pal, palmitate; Ste, stearate; TOC, Total organic carbon; For, formate; Ace, acetate; Pro, propionate; Oxa, oxalate.

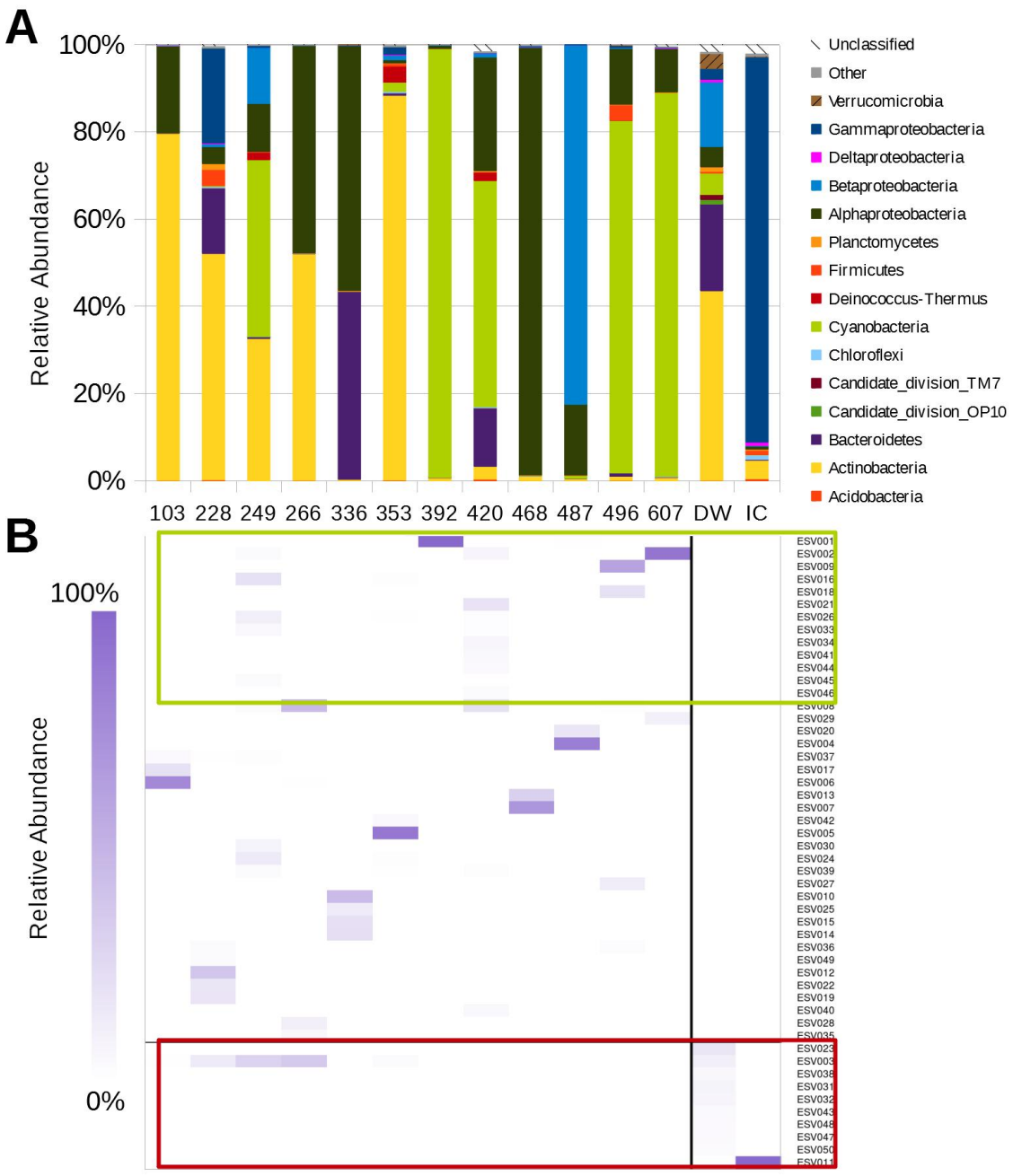

Fig. S3

A) Taxonomic composition at the phylum level with Proteobacteria expanded into classes. Sample names indicate sampling depth, except in DW (drilling water control) and IC (internal laboratory control). **B)** Distribution of the 50 most abundant Exact Sequence Variants (ESVs). The green rectangle indicates the ESVs belonging to the Cyanobacteria phylum. The red rectangle indicates the ESVs that were present in at least one of the two contamination controls.

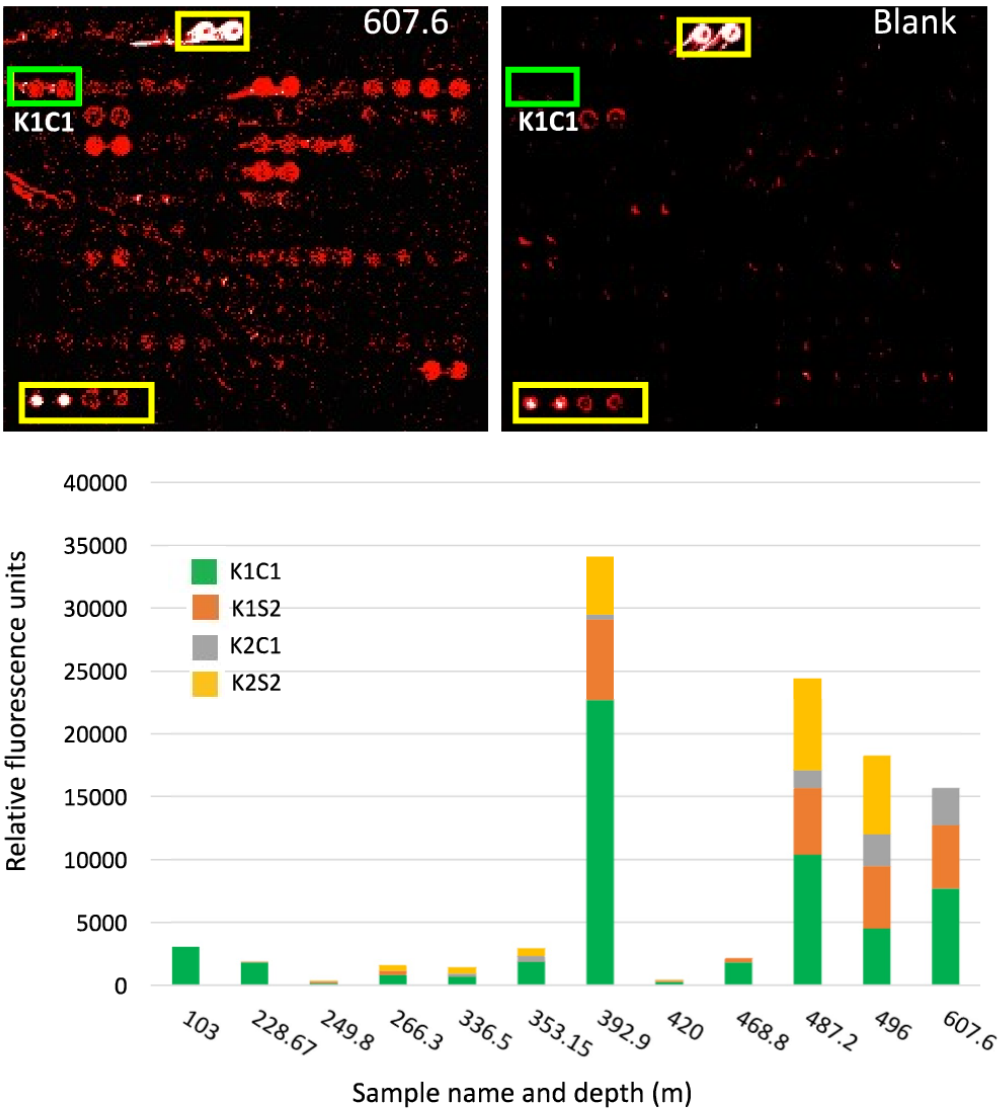

Fig. S4

LDChip, A life detector antibody microarray chip detected cyanobacterial markers in deep core samples. C.a. 0.5 g of sample was grounded with a mortar and pestle and analyzed by a multiplex fluorescent microarray immunoassay with LDChip (see Methods). Partial LDChip microarray image obtained with sample 607.6 and the corresponding blank section (top) showing fluorescence signal in the duplicated spots corresponding to antibody K1C1 against the type cyanobacterial strain *Anabaena* sp. PCC7120 (order Nostocales). Chart showing the sum of the fluorescence intensities of the four anti-cyanobacteria antibodies present on the LDChip after assaying the different samples analysed in this work: K1C1 and K1S2 are antibodies against *Anabaena* cells and exopolymeric fraction, respectively, grown in the presence of nitrate; K2C1 and K2S2, are against *Anabaena* grown in the absence of nitrate, that is, under nitrogen fixation conditions. Yellow rectangles indicate fluorescent frame markers. Red spots correspond to positive immunodetections with the corresponding antibodies.

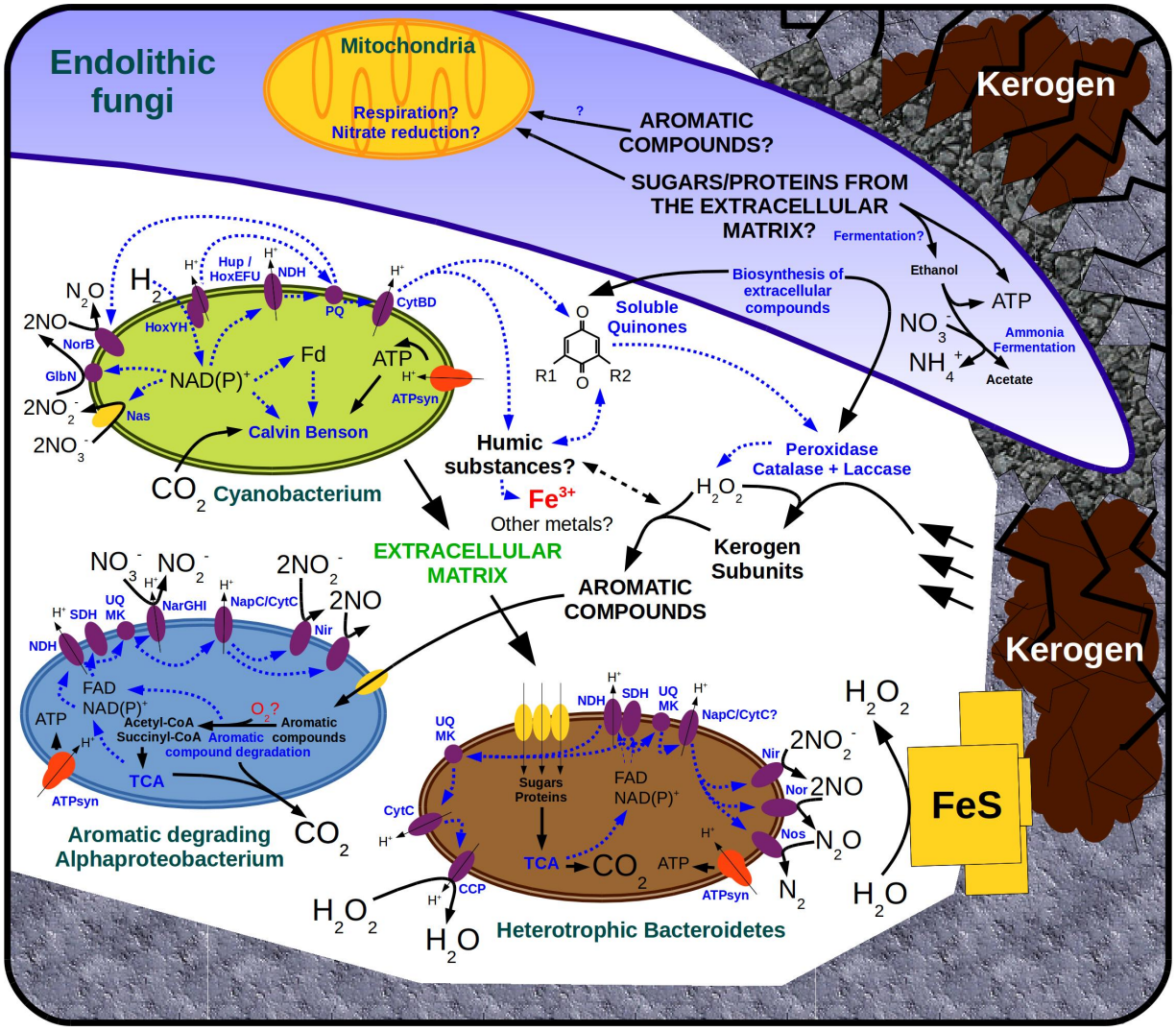

Fig. S5

Potential metabolic interactions in the microbial community found in sample 420. Names in blue correspond to enzymes, electron carriers or metabolic pathways; names in black correspond to organic and inorganic compounds. Dotted blue arrows correspond to electron flow; black arrows correspond to mass flow. Dotted black arrows or names with interrogations indicate processes that have been described in the literature but are not directly supported by the metagenomic data. Abbreviations: ATPsyn, ATP synthase; CCP, cytochrome C peroxidase; cytBD, cytochrome bd; cytC, cytochrome C; Fd, ferredoxin; FDH, formate dehydrogenase; glbN, cyanoglobin, hup, uptake hydrogenase; hox, bidirectional hydrogenase; MK, menaquinone; napC/cytC, denitrification associated cytochrome C; nar, respiratoty nitrate reductase; NDH, NADH dehydrogenase; nir, respiratoty nitrite reductase; nor, respiratory nitric oxide reductase; nos, nitrous oxide reductase; PQ, plastoquinone; SDH, succinate dehydrogenase; TCA, tricarboxylic acid cycle; UQ, ubiquinone.

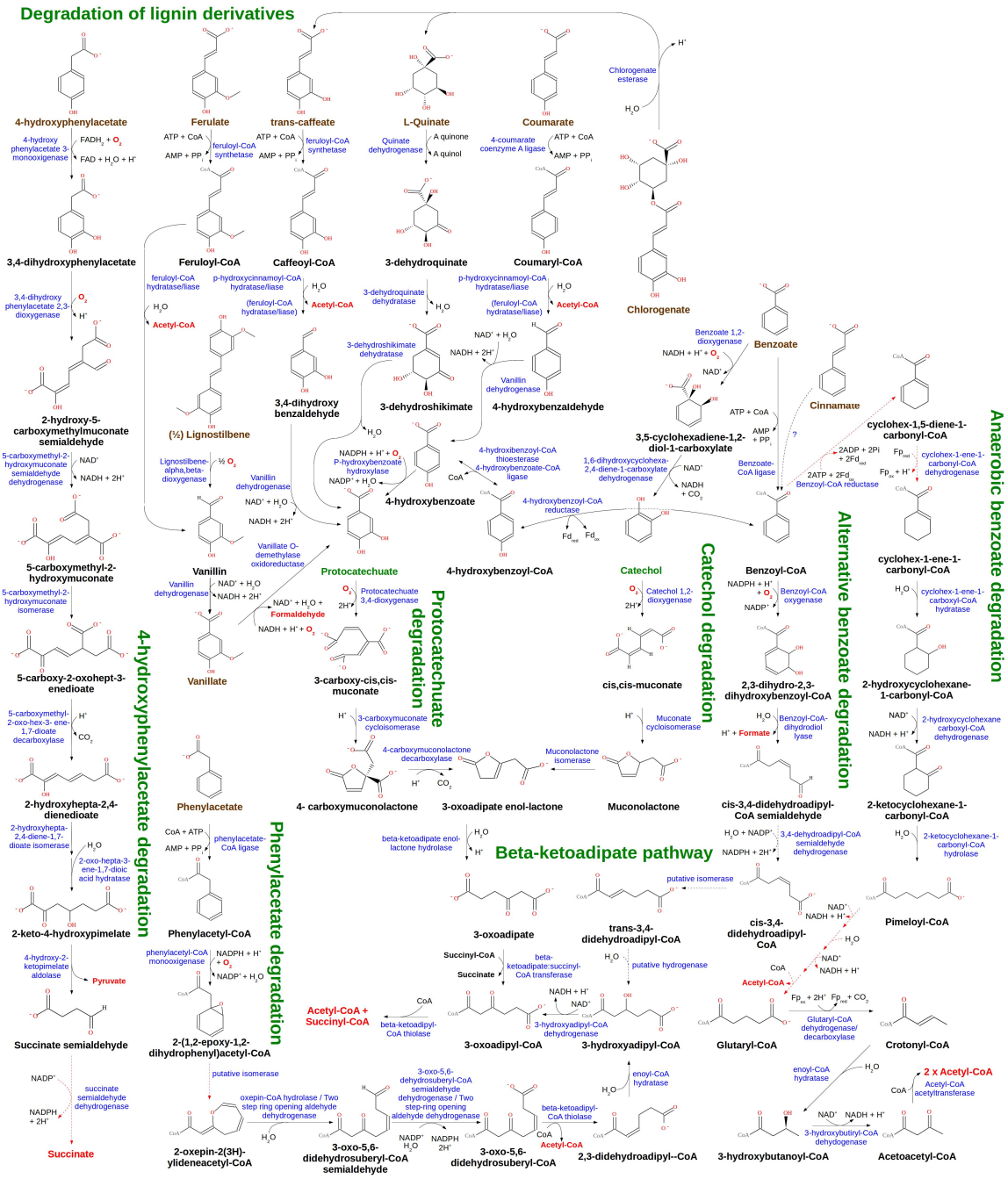

Fig. S6

Metabolic pathways for the degradation of lignin derivatives and other aromatic compounds found in the metagenome of sample 420. Red dashed arrows indicate reactions not directly supported by the metagenomic data.

	Ultra-Clean Soil DNA 0.5g isolation	Ultra-Clean Soil DNA 2 10 x 0.5 g isolation	PowerMax Soil DNA Up to 10g isolation
BH10-103	✓	---	---
BH10-228	✓	---	---
BH10-249	✓	---	---
BH10-266	✓	---	---
BH10-336	---	✓	---
BH10-353	---	---	✓
BH10-392	---	✓	---
BH10-420	✓	---	---
BH10-468	---	---	✓
BH10-487	---	---	✓
BH10-496	✓	---	---
BH10-607	---	✓	---

Table S1.
DNA isolation methods used for each of the rock core samples.

	420	607
Raw reads	254,722,502	290,849,322
Normalized reads (MG-RAST)	75,381,844	22,302,242
Contigs	438,065	15,641
Assembly size (Mb)	542.97	18.79
Maximum contig length	963,668	16,857
N50	2,814	1,941
Reads mapping to contigs	242,595,714	285,073,318
Coverage	45.13x	1532.52x

Table S2.
Metagenomic sequencing and assembly statistics

Data S1. (separate file)

Single-nucleotide resolution 16S rRNA-based taxonomic composition of the samples analyzed in this study.

Data S2. (separate file)

Subsystem-based annotation of the metagenomic reads from samples 420 and 607.

References

1. Abed R, Lam P, De Beer D, Stief P (2013). High rates of denitrification and nitrous oxide emission in arid biological soil crusts from the Sultanate of Oman. *ISME J* 7:1862-1875.
2. Gadd GM (2017). New horizons in geomycology. *Environ Microbiol Rep* 9:4–7.
3. Borda MJ, Elsetinow AR, Schoonen MA, Strongin DR (2001). Pyrite-induced hydrogen peroxide formation as a driving force in the evolution of photosynthetic organisms on an early Earth. *Astrobiology* 1:283-288.
4. Lim YW, Baik KS, Han SK, Kim SB, Bae KS (2003). *Burkholderia sordidicola* sp. nov., isolated from the white-rot fungus *Phanerochaete sordida*. *Int J Syst Evol Microbiol* 53:1631-1636.
5. Neal JL, Allen GC, Morse RD, Wolf DD (1983). Nitrate, nitrite, nitrous oxide and oxygen-dependent hydrogen uptake by Rhizobium. *FEMS Microbiol Lett* 17:335-338.
6. Cole JK et al. (2014). Phototrophic biofilm assembly in microbial-mat-derived unicyanobacterial consortia: model systems for the study of autotroph-heterotroph interactions. *Front Microbiol* 5.
7. Mazor G, Kidron GJ, Vonshak A, Abeliovich A (1996). The role of cyanobacterial exopolysaccharides in structuring desert microbial crusts. *FEMS Microbiol Ecol* 21:121-130.